


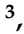




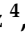


## Article

# Mapping the Future: Climate-Induced Changes in Aboveground Live-Biomass Carbon Density Across Mexico's Coniferous Forests

Carmela Sandoval-García <sup>1</sup>, Jorge Méndez-González <sup>1,\*</sup>, Flores Andrés <sup>2</sup>,  
Eulalia Edith Villavicencio-Gutiérrez <sup>3</sup>, Fernando Paz-Pellat <sup>4</sup>,  
Celestino Flores-López <sup>1</sup>,  
Eladio Heriberto Cornejo-Oviedo <sup>1</sup>, Alejandro Zermeño-González <sup>5</sup>, Librado Sosa-Díaz <sup>4</sup>,  
Marino García-Guzmán <sup>1</sup> and José Ángel Villarreal-Quintanilla <sup>6</sup>

- <sup>1</sup> Department of Forestry, Autonomous Agrarian University Antonio Narro, Calz. Antonio Narro 1923, Saltillo 25315, Coahuila, Mexico; ka\_rmen7@hotmail.com (C.S.-G.)
- <sup>2</sup> National Center for Disciplinary Research in Conservation and Improvement of Forest Ecosystems, National Institute for Forestry, Agriculture and Livestock Research, Progreso 5, Mexico City 04010, Coyoacán, Mexico; flores.andres@inifap.gob.mx
- <sup>3</sup> National Institute for Forestry, Agriculture and Livestock Research, Progreso 5, Saltillo Experimental Station, Saltillo 25315, Coahuila, Mexico
- <sup>4</sup> Postgraduate College, Campus Montecillo, Montecillo, Texcoco 56264, Edo. de México, Mexico
- <sup>5</sup> Irrigation and Drainage Department, Autonomous Agrarian University, Antonio Narro. Calz. Antonio Narro 1923, Saltillo 25315, Coahuila, Mexico
- <sup>6</sup> Department of Botany, Autonomous Agrarian University Antonio Narro, Calz. Antonio Narro 1923, Saltillo 25315, Coahuila, Mexico
- \* Correspondence: jmendezg@hotmail.com; Tel.: +52-84431-21141



**Citation:** Sandoval-García, C.; Méndez-González, J.; Andrés, F.; Villavicencio-Gutiérrez, E.E.; Paz-Pellat, F.; Flores-López, C.; Cornejo-Oviedo, E.H.; Zermeño-González, A.; Sosa-Díaz, L.; García-Guzmán, M.; et al. Mapping the Future: Climate-Induced Changes in Aboveground Live-Biomass Carbon Density Across Mexico's Coniferous Forests. *Forests* **2024**, *15*, 2032. <https://doi.org/10.3390/f15112032>

Academic Editors: Cheng Li, Fei Zhang, Mou Leong Tan and Kwok Pan Chun

Received: 7 October 2024  
Revised: 11 November 2024  
Accepted: 15 November 2024  
Published: 18 November 2024



**Copyright:** © 2024 by the authors. Licensee MDPI, Basel, Switzerland. This article is an open access article distributed under the terms and conditions of the Creative Commons Attribution (CC BY) license (<https://creativecommons.org/licenses/by/4.0/>).

**Abstract:** Climate variations in temperature and precipitation significantly impact forest productivity. Precipitation influences the physiology and growth of species, while temperature regulates photosynthesis, respiration, and transpiration. This study developed bioclimatic models to assess how climate change will affect the carbon density of aboveground biomass ( $_{cd}AGB$ ) in Mexico's coniferous forests for 2050 and 2070. We used  $_{cd}AGB$  data from the National Forest and Soils Inventory (INFyS) of Mexico and 19 bioclimatic variables from WorldClim ver. 2.0. The best predictors of  $_{cd}AGB$  were obtained using machine learning techniques with the “caret” library in R. The model was trained with 80% of the data and validated with the remaining 20% using Generalized Linear Models (GLMs). Current  $_{cd}AGB$  prediction maps were generated using the best predictors. Future  $_{cd}AGB$  was calculated with the average of three general circulation models (GCMs) of future climate projections from the Coupled Model Intercomparison Project Phase 5 (CMIP5), under four Representative Concentration Pathways (RCPs): 2.6, 4.5, 6.0, and 8.5  $W/m^2$ . The results indicate  $_{cd}AGB$  losses in all climate scenarios, reaching up to 15  $Mg\ C\ ha^{-1}$ , and could occur under the RCP 8.5 scenario by 2070 in the central region of the country. Temperature-related variables are more important than precipitation variables. Bioclimatic variables can explain up to 20% of the total variance in  $_{cd}AGB$ . The temperature in the study area is expected to increase by 2.66 °C by 2050 and 3.36 °C by 2070, while precipitation is expected to fluctuate by  $\pm 10\%$  relative to the current values, which could geographically redistribute the  $_{cd}AGB$  of the country's coniferous forests. These findings underscore the need for forest management to focus not only on biodiversity conservation but also on the carbon storage capacity of these ecosystems.

**Keywords:** aboveground biomass; bioclimatic models; climate change; coniferous forests; machine learning

## 1. Introduction

Forests occupy approximately 31% of the Earth's terrestrial surface, equivalent to around 4.06 billion hectares, and play a pivotal role in climate regulation by acting as major

carbon sinks. Global forests are estimated to sequester approximately 662 gigatonnes (Gt) of carbon, distributed as follows: 44% in living biomass, 45% in soil organic matter, and 11% in dead wood and litter [1].

In Mexico, forests cover approximately 64.8 million hectares, accounting for about 33% of the national land area [1]. These forests include a wide range of types, including temperate, broad-leaved, mixed, and tropical forests [2], and are estimated to store around 1.69 Gt of carbon [3]. Changes in temperature and precipitation patterns due to climate change have been shown to adversely affect forest growth, biomass accumulation, and carbon sequestration at a global scale [4,5].

The scientific basis for studying climate change is unequivocal, and the findings are irrefutable; climate change is present and highly likely to intensify in the coming years. Between 2011 and 2020, the global average surface temperature rose by 1.09 °C compared to the 1850–1900 baseline, with more pronounced warming observed in the Northern Hemisphere, particularly over land (1.59 °C) compared to oceans (0.88 °C). Precipitation patterns are shifting, with increases observed at higher latitudes and decreases in the subtropics. Climate projections indicate that extreme events will escalate in frequency and intensity, while the carbon sequestration capacity of global forest ecosystems is projected to diminish [6].

In Mexico, the average temperature increased by 0.31 °C per decade between 1971 and 2020, with the most pronounced effects occurring in the northern plateau during the summer months. According to projections under the SSP3-7.0 climate scenario, the average temperature is expected to increase by 0.82 °C between 2020 and 2039 and by 1.63 °C between 2040 and 2059. In addition, some northern states are likely to experience significant reductions in precipitation [7].

Precipitation and temperature are well established as primary drivers of forest biomass productivity [4]. Precipitation plays a pivotal role in plant physiology by regulating transpiration, nutrient uptake, stomatal conductance, and nutrient availability [8,9]. In addition to shaping species-specific growth strategies. Variations in precipitation availability also affect water use efficiency [10,11], with a direct relationship between precipitation levels and biomass productivity [2].

Similarly, temperature exerts significant control over plant growth by modulating fundamental physiological processes, including photosynthesis, respiration, and transpiration [4,12]. It also governs the rate of chemical reactions and CO<sub>2</sub> assimilation [13]. While rising temperatures may stimulate biomass accumulation in boreal forests, they tend to suppress growth in tropical forests [14]. Excessively high temperatures reduce growth rates, alter leaf pigmentation, impair root system development, and induce water stress, thereby disrupting normal growth patterns [15].

Plants from temperate climates exhibit a degree of cold tolerance, but extremely low temperatures negatively affect processes such as cell division, photosynthesis, and metabolic activity, leading to reduced productivity [16].

Climatic variations are driving forests to become increasingly dynamic systems [17], resulting in changes in tree species composition within ecosystems [11]. Simultaneous shifts in temperature and precipitation lead to either reductions or increases in ecosystem biomass, thereby altering global forest distribution patterns [18].

It is well established that temperature exerts both positive and negative effects on aboveground forest biomass [4,19,20]. Furthermore, annual precipitation is generally positively correlated with aboveground biomass [12,21], though this relationship is not fully consistent, as it depends on forest type and, more importantly, the specific bioclimatic variable being correlated [22]. These effects have been documented across various forest biomes, including temperate, tropical, and boreal ecosystems [14], as well as at the species level [8].

To estimate aboveground biomass in forest ecosystems, both dynamic variables (related to climate) and static variables (such as diameter at breast height, basal area, stand density, slope, aspect, and elevation, among others) have been jointly applied [8,23–25].

These mixed models, incorporating dynamic and static variables that influence above-ground biomass, demonstrate predictive capacities ranging from moderate ( $R^2 = 0.19$ ) to very high ( $R^2 = 0.86$ ), as indicated by their determination coefficients [8,23,24]. In some cases, these models include nine or more explanatory variables [8].

While these models are useful for identifying correlations between biomass and environmental variables, they are limited in their ability to quantify the direct impacts of climate change on aboveground biomass [8,23,26].

To effectively assess the impact of climate change on carbon density across different scales (species, genus, ecosystems), it is essential to use dynamic variables. Moreover, focusing on dynamic variables provides insights into how potential future climate fluctuations, in both temperature and precipitation, will affect carbon density. This supports effective forest management and informed conservation policies while facilitating the development of adaptive strategies to address the challenges posed by climate change.

Furthermore, forests are highly dynamic systems that undergo temporal changes due to natural disturbances, anthropogenic activities, and climatic fluctuations, which introduces additional complexity to the modeling process [25,27].

The research conducted by [22] indicated that, among ten conifer species, precipitation demonstrated a positive correlation with aboveground biomass density ( $0 \leq \rho \leq 0.20$ ), whereas temperature exhibited a negative correlation ( $-0.20 \leq \rho \leq 0$ ). Importantly, the magnitude and direction of the correlation between climatic variables and aboveground biomass in forest ecosystems are highly contingent upon several factors, such as spatial scale [28], forest type [4], and species-specific traits [12,23].

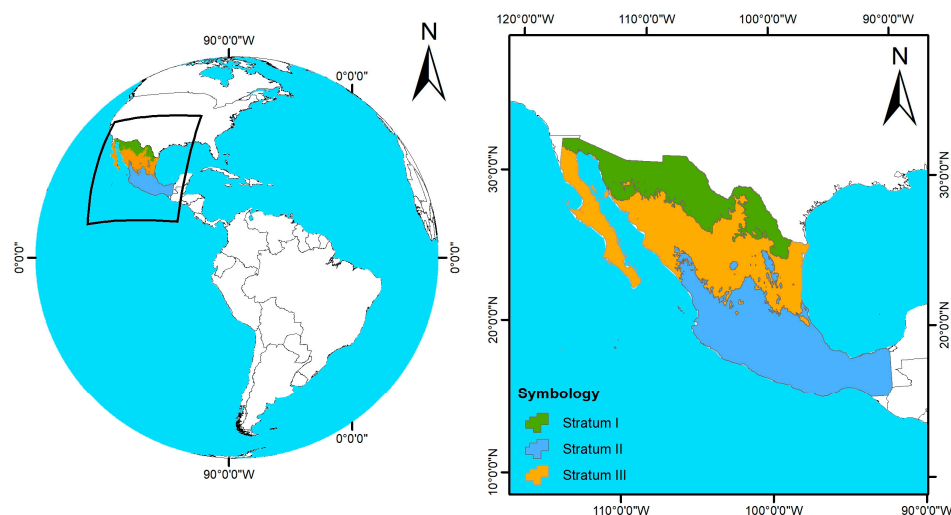
To deepen our understanding of how climate change specifically influences above-ground biomass, it is imperative to develop new modeling frameworks. These models should integrate dynamic climatic data to directly assess the effects of climate variability and enable future projections—an objective that cannot be fully achieved by models that rely solely on static stand or site-level variables.

Based on the above considerations, the primary objective of this study was to develop bioclimatic models specifically designed to assess the impact of climate change on the geospatial distribution of aboveground live biomass carbon density in Mexican pine forests. Bioclimatic models are defined as predictive tools that assess the relationships between climatic variables and biological responses. These models can be based on climatic variables alone or in conjunction with additional non-climatic covariates [29]. The analysis incorporated four distinct climate scenarios based on Representative Concentration Pathways (RCPs) 2.6, 4.5, 6.0, and 8.5  $W/m^2$ , projected for 2050 and 2070. These models are intended to provide highly accurate information that can enhance forest management practices and contribute to climate change mitigation efforts. It is hypothesized that future climate projections will exert a significant influence on the aboveground biomass carbon density in the pine forests of Mexico.

## 2. Materials and Methods

### 2.1. Study Area Description

Conifers in Mexico are found from sea level up to over 4000 m in altitude, with the highest diversity concentrated in the Sierra Madre Occidental (SMOc) and the Sierra Madre Oriental (SMO), and Mexico hosts 49 species of pine, representing 40% of the approximately 120 pine species worldwide [30]. The distribution of these species spans approximately from 32 °N north latitude to 19 °N and from 105 °W west longitude to 98 °W on soils derived from igneous and metamorphic rocks [31]. These ecosystems are characterized by a climate with cold temperatures, with annual precipitation ranging from 350 to 1200 mm and average temperatures ranging from 6 to 28 °C [32] and with rainy summers and dry, cold winters, and they are dominated by coniferous trees such as pines (*Pinus* spp.), firs (*Abies* spp.), cedars (*Cupressus* spp.), and junipers (*Juniperus* spp.) [33] (Figure 1).



**Figure 1.** Study area in the global context (left) and regional context (right).

## 2.2. Data Acquisition and Cleaning Process

A total of 22 parameters, including type, topographic, species richness, biomass, carbon (aboveground and belowground), health indices, climate, geographic, and dasometric factors (Appendix A), were obtained from [2]. From there, we used data on carbon density in aboveground live biomass (henceforth referred to as  $cdAGB$ ), geographic coordinates (lat, long), and ID of each cluster, exclusively from the parameter type = “coniferous forests”. The  $cdAGB$  is the carbon stock per unit area of live biomass contained in living trees, including stems, branches, leaves, and seeds [34]. These data were calculated from the National Forest and Soil Inventory (INFyS) of Mexico (2009–2012) [2]. Additionally, we utilized 19 bioclimatic variables from WorldClim version 2.0, covering the period from 1970 to 2000 (Appendix B), in raster format with a resolution of 30 arcseconds, published in January 2020 [35]. These variables have been previously used in similar studies [8,9,12,14,28,36].

Using the “raster” library in R [37], we employed the geographic coordinates of each cluster to extract values for the 19 bioclimatic variables (Bios). To identify erroneous or atypical data in  $cdAGB$ , we applied a Principal Component Analysis (PCA) to the centered and scaled matrix of  $cdAGB$  and 19 Bios, using the “FactoMineR” v.2.9 library [38]. We considered outliers as those falling outside the 95% confidence ellipse of the PCA, which were subsequently excluded from the dataset to ensure the coherence and reliability of the results.

## 2.3. Predictive Modeling of $cdAGB$

Due to the significant climatic variability recorded in the pine forests of the country [31], and in order to enhance predictions of  $cdAGB$ , a bioclimatic stratification of Mexico’s pine forest areas was conducted. We utilized 19 bioclimatic variables in raster format, employing the “GeoStratR” library [39], to create strata (geographical space) in the same format. The clusters from INFyS located within each generated stratum were separated for independent analysis.

For the selection of predictors (Bios) of  $cdAGB$ , within each stratum, the machine learning (ML) technique employing 10-fold cross-validation was utilized, employing backward selection. A tuning grid ranging from 1 to 7 predictors (nvmax = 1:7) was considered [40]. The statistical significance of regression coefficients ( $p < 0.05$ ) and the variance inflation factor (VIF) were evaluated to mitigate multicollinearity effects.

With the subset of predictors that met these criteria, the model was trained using the Generalized Linear Models (GLMs) method with the “identity” link function. For this purpose, 80% of the data (randomly obtained and by quantiles) were used. This approach (GLM) is suitable for continuous and positive response variables [2,9] in this type of study.



The model fitting was performed using the “caret” package in R [40]. Hypothesis tests ( $\alpha = 0.05$ ) were conducted on the regression coefficients ( $H_0 : \beta_i = 0$  vs  $H_1 : \beta_i \neq 0, \dots, \beta_{ij}$ ) of the final model. We utilized the “lmg” metric to calculate the importance of each bioclimatic variable (as a percentage of the variance explained by the model), which provides a decomposition of the model’s explained variance into non-negative contributions [41]. For the remaining 20% of the data, the model was validated using various techniques: Leave-One-Out Cross-Validation (LOOCV), Cross-Validation (CV;  $k = 10$ ), Repeated Cross-Validation (RCV,  $k = 10$ ,  $\text{rep} = 10$ ), and Bootstrap (reps = 100). The evaluation included calculations of Root Mean Square Error (RMSE), Pseudo Coefficient of Determination (Rsquared), and Mean Absolute Error (MAE) to assess the model’s performance. These validations were conducted using the “caret” R package [40].

#### 2.4. Current and Future Prediction and Rate of Change of $_{cd}AGB$

Using the generated bioclimatic models, current predictions of  $_{cd}AGB$  were made for each stratum, employing the corresponding bioclimatic predictors. The raster library in R software [37] was used to predict  $_{cd}AGB$  values. Specifically, we applied the argument type = “response”—a function within the raster library—to generate  $_{cd}AGB$  prediction maps in raster format. This approach enabled the creation of spatially explicit maps that visualize the distribution and magnitude of predicted variables across the study area.

To predict future  $_{cd}AGB$ , raster layers from three different General Circulation Models (GCMs) were obtained: MIROC-6, GISS-E2, and CMCC-ESM2. From these models, only the bioclimatic predictors of  $_{cd}AGB$  for each stratum were selected. The GCMs are derived from future climate projections of the Coupled Model Intercomparison Project Phase 5 (CMIP5) at a resolution of 2.5 degrees. Four Representative Concentration Pathways (RCPs) developed by the Intergovernmental Panel on Climate Change [42] were used, characterized by their projected Total Radiative Forcing (TRF) for the year 2100, ranging from 2.6, 4.5, and 6.0 to 8.5  $W/m^2$ , considering the years 2050 and 2070. These RCP scenarios are used to project potential future trajectories of climate change based on different emission levels and mitigation efforts.

The three layers of each GCM, RCP, and year were averaged using raster algebra. Using this average and the corresponding bioclimatic model, future prediction of  $_{cd}AGB$  was conducted for each stratum. Similarly, the R raster library [37] was employed with the argument type = “response” to generate raster maps of future  $_{cd}AGB$  predictions. To identify changes in future  $_{cd}AGB$  relative to the current scenario, the following expression was employed:  $_{cd}AGB$  (future)  $-$   $_{cd}AGB$  (current). The results are as follows: 0 if pixel values are equal in both scenarios; positive if  $_{cd}AGB$  is higher in the future; and negative if  $_{cd}AGB$  is higher in the current scenario.

To visualize the vulnerable areas of Mexico’s coniferous forests to changes in  $_{cd}AGB$  due to climate change, a 40 km radius buffer was created around each site from the National Forest and Soil Inventory. This delineated the forested areas that were potentially affected. Subsequently, the number of pixels for each  $_{cd}AGB$  change category or rate within these buffer polygons was quantified. The resulting change rate was then presented in map form for each RCP and year.

In addition, uncertainty in future predictions of  $_{cd}AGB$  was quantified using the standard error:  $EE(\theta) = \sqrt{[\text{Var}(\theta)]}$ . This involved repeated predictions of  $_{cd}AGB$  from MIROC-6 + GISS-E2 + CMCC-ESM2, for each RCP and year, which were averaged using the raster library [37], and generating a raster map of  $EE(\theta)$ .

#### 2.5. Bioclimatic Predictors: Current Analysis and Future Projections

In order to determine the influence of future bioclimatic predictors on the changes in  $_{cd}AGB$  of Mexican forests, the non-parametric Wilcoxon signed-rank test was employed. This test was used to evaluate whether there are significant differences between the medians of two samples: the current bioclimatic predictor and the future bioclimatic predictor (e.g., current Bio1 vs. Bio1 2050, RCP 4.0). A significance level of 95% was used.

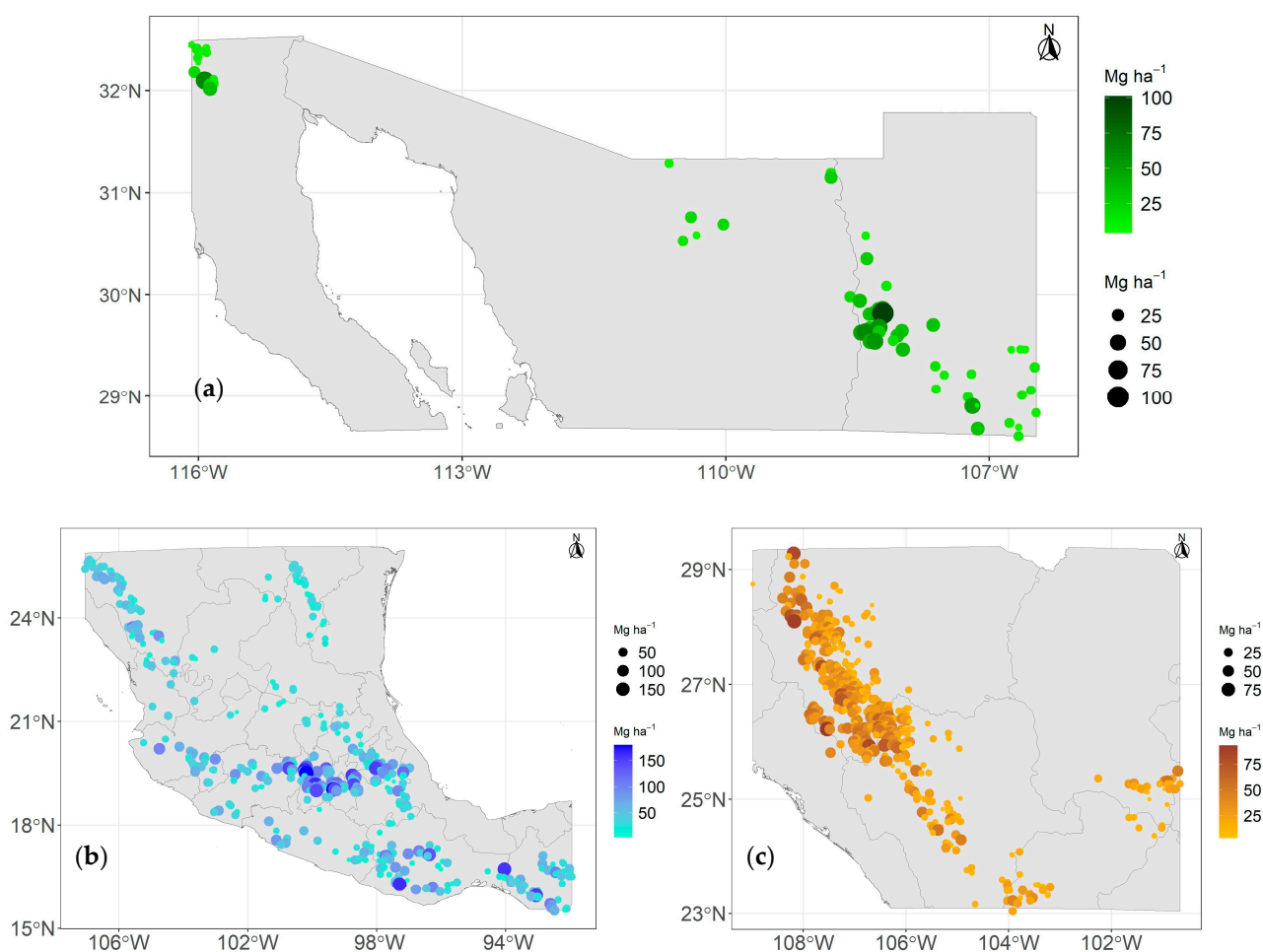
For this purpose, the current and future values (average of 3 GCMs, RCP, and year) of the predictors for each stratum (Bios) were extracted the geographic coordinates of each cluster and employing the raster library [37]. These analyses were represented in violin plots, with temperature-derived Bios shown in orange and precipitation-derived Bios in blue, with statistical significance indicated by the \* symbol at the top.

All statistical analyses, figures, and geographic processing were performed using R software version 4.3.1 [43].

### 3. Results

#### 3.1. Distribution Carbon Density of Aboveground Live Biomass

The stratification process of the coniferous forests in Mexico resulted in three strata: stratum I, located in the northwest of the country (Figure 2a;  $n = 60$ ), stratum II, in the central-southern part of the country (Figure 2b;  $n = 450$ ), and stratum III, located in the Sierra Madre Occidental, SMO (Figure 2c;  $n = 463$ ). The sample size for each stratum varies, as indicated in Table 1. This variation is determined by the geographic extent of each stratum generated during the stratification process and by the number of National Forest and Soil Inventory sites located within each stratum.



**Figure 2.** Distribution of sites from the National Forest and Soil Inventory (2009–2012): stratum I (a), stratum II (b), and stratum III (c). The size of the circles and the color gradient indicate the values of carbon density in the aboveground live biomass (Mg C ha<sup>-1</sup>).

**Table 1.** Regression coefficients for the prediction of the carbon density of aboveground live biomass by stratum in the coniferous forests of Mexico.

Stratum	Coefficient	Estimate	95% CI		Std. Err	T Value	Pr (> t )	Residual Deviance	VIF	Imp. (%)
			2.5	97.5						
I (n = 48)	β <sub>0</sub> (intercept)	64.8332	22.7606	97.3943	23.2221	2.79	0.00772 **	13.246	1.02	10.33
	β <sub>1</sub> (Bio 5)	−0.1897	−0.2932	−0.0544	0.0737	−2.57	0.01355 *			
	β <sub>2</sub> (Bio 18)	0.0586	0.0337	0.0829	0.0123	4.77	2.02 × 10 <sup>−5</sup> ***			
II (n = 360)	β <sub>0</sub> (intercept)	87.6362	66.3661	108.9076	10.4558	8.38	1.22 × 10 <sup>−15</sup> ***	172.17	1.03	8.04
	β <sub>1</sub> (Bio 5)	−0.2572	−0.3296	−0.1841	0.0376	−6.84	3.37 × 10 <sup>−11</sup> ***			
	β <sub>2</sub> (Bio 12)	0.0190	0.0106	0.0272	0.0037	5.12	4.91 × 10 <sup>−7</sup> ***			
III (n = 370)	β <sub>0</sub> (intercept)	26.6379	12.3682	40.4383	8.4994	3.13	0.00186 **	132.39	1.16	3.28
	β <sub>1</sub> (Bio 10)	−0.0959	−0.1571	−0.0293	0.0391	−2.45	0.01461 *			
	β <sub>2</sub> (Bio 13)	0.0933	0.0708	0.1160	0.0135	6.93	1.8 × 10 <sup>−11</sup> ***			

β<sub>0</sub>, β<sub>1</sub>, and β<sub>2</sub>: are the regression coefficients; 2.5 and 97.5: 95% confidence intervals of the regression coefficients; Std. Err: standard error of the regression coefficients; Pr (>|t|): The probability of obtaining a T-value more extreme than the observed one, assuming that the null hypothesis is true. VIF: variance inflation factor; Imp = importance value of the variables. Bio 05: Max Temperature of Warmest Month (°C); Bio 10: Mean Temperature of Warmest Quarter (°C); Bio 12: Annual Precipitation (mm); Bio 13: Precipitation of Wettest Month (mm); Bio 18: Precipitation of Warmest Quarter (mm). Statistical significance: “\* p < 0.05”: Significant; “\*\* p < 0.01”: Highly significant; “\*\*\* p < 0.001”: Very highly significant.

### 3.2. Models for Predicting Carbon Density in the Aboveground Live Biomass

The bioclimatic variables selected by the algorithms were statistically significant (p < 0.05) for predicting *cd*AGB. The predictors (Bios) of *cd*AGB were represented by both precipitation variables (3 out of 6) and temperature variables (3 out of 6). However, at the stratum level, temperature variables were more important (Imp., Table 1) than precipitation variables. Bio 5 (Max Temperature of Warmest Month) was the best predictor of *cd*AGB in strata I and II. No model exhibited multicollinearity (VIF < 1.16), which ensures that *cd*AGB predictions are not overestimated.

The equations for estimating *cd*AGB in each stratum are as follows:

$$\text{Stratum I: } cdAGB \text{ (Mg C ha}^{-1}\text{)} = 64.8332 + -0.1897 \times \text{Bio 5 (}^{\circ}\text{C} \times 10\text{)} + 0.0586 \times \text{Bio 18 (mm)} \tag{1}$$

$$\text{Stratum II: } cdAGB \text{ (Mg C ha}^{-1}\text{)} = 87.6362 + -0.2572 \times \text{Bio 5 (}^{\circ}\text{C} \times 10\text{)} + 0.0190 \times \text{Bio 12 (mm)} \tag{2}$$

$$\text{Stratum III: } cdAGB \text{ (Mg C ha}^{-1}\text{)} = 26.6379 + -0.0959 \times \text{Bio 10 (}^{\circ}\text{C} \times 10\text{)} + 0.0933 \times \text{Bio 13 (mm)} \tag{3}$$

The mean of *cd*AGB does not follow a pattern among strata; that is, it is not lower in stratum I and higher in stratum III. The mean *cd*AGB in stratum II represents, on average, up to 1.6 times more than in strata I and III; and it ranges from 23.14 Mg C ha<sup>−1</sup> (stratum I) to 42.57 Mg C ha<sup>−1</sup> (stratum II), with maximum values reaching almost 180 Mg C ha<sup>−1</sup> (Table 2), but it also has the highest variability (CV > 60%). None of the variables showed normality (p < 0.0001) according to the Shapiro–Wilk and Anderson–Darling tests (Table 2).

**Table 2.** Descriptive statistics of the observed carbon density of aboveground live biomass and its predictors (1950–2000 period) in the coniferous forests of Mexico.

Stratum	Parameter	n	Min	P25	Mean	Median	P75	Max	SD	CV	Shapiro	Anderson
											p-Value	p-Value
I	<i>cd</i> AGB	48	4.23	11.54	23.14	16.23	33.35	62.05	15.04	65	0.0001	0.0001
	Bio 5		27.7	28.7	29.97	29.6	30.75	36	1.76	5.89	0.0001	0.0001
	Bio 18		62	223	256.89	290	330.5	397	101.66	39.57	0.0001	0.0001
II	<i>cd</i> AGB	360	4.46	19.87	42.57	34.35	54.75	179.69	33.01	77.54	0.0001	0.0001
	Bio 5		17.5	22.78	25.72	25.3	28.7	34.6	3.93	15.28	0.0001	0.0001
	Bio 12		426	895.25	1109.42	1092	1314.25	2216	367.25	33.1	0.0001	0.0001

Table 2. Cont.

Stratum	Parameter	<i>n</i>	Min	P25	Mean	Median	P75	Max	SD	CV	Shapiro	Anderson
											<i>p</i> -Value	<i>p</i> -Value
III	cdAGB	370	3.15	12.76	26.26	23.24	35.98	92.92	16.56	63.05	0.0001	0.0001
	Bio 10		14.7	17.4	18.55	18.3	19.4	26.3	1.74	9.39	0.0001	0.0001
	Bio13		53	154	184.03	181	219	357	52.54	28.55	0.0001	0.0001

cdAGB: carbon density of aboveground live biomass (Mg C ha<sup>-1</sup>); Bio 5: Max Temperature of Warmest Month (°C); Bio18: Precipitation of Warmest Quarter (mm); Bio12: Annual Precipitation (mm); Bio10: Mean Temperature of Warmest Quarter (°C); Bio13: Precipitation of Wettest Month (mm); *n* = number of sites in the stratum; Min: minimum value; P25 and P75: 25th and 75th percentiles; Max: maximum value; SD: standard deviation; CV: coefficient of variation (%).

### 3.3. Validation of Predictive Models for cdAGB

According to the pseudo R<sup>2</sup> derived from the validation procedure, bioclimatic variables explain an average of 19% of the cdAGB (Table 3). The LOOCV method calculates the lowest R<sup>2</sup> (0.10), while the other methods yield an average R<sup>2</sup> of 0.22. According to the validation, when using the models to predict aboveground biomass carbon density with independent data from the training set, the estimation errors (RMSE) could range from 13.18 Mg C ha<sup>-1</sup> (stratum III) to 42.42 Mg C ha<sup>-1</sup> (stratum I), with the best estimates observed in stratum III.

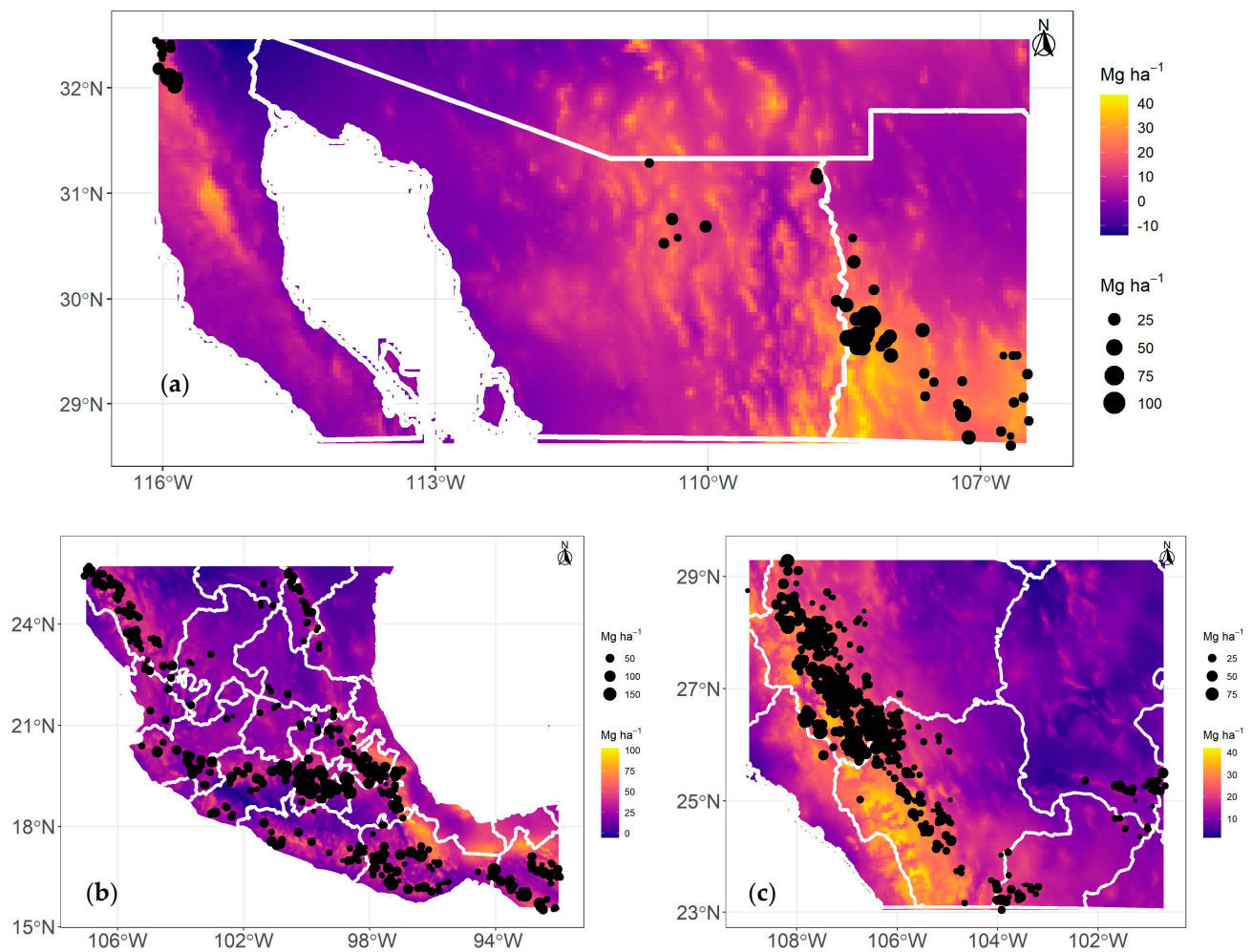
**Table 3.** Validation of bioclimatic regression models for predicting the carbon density of aboveground live biomass in coniferous forests in Mexico.

Stratum	Method	Set	<i>n</i>	Pseudo R <sup>2</sup>	RMSE	MAE
I	LOOCV	Training	48			
		Validation	12	0.031	38.319	30.806
	CV	Validation	12	0.177	29.908	29.379
	RCV	Validation	12	0.177	31.949	31.272
II	Bootstrap	Validation	12	0.316	42.426	34.457
	LOOCV	Training	360			
		Validation	90	0.128	29.938	21.789
	CV	Validation	90	0.249	28.493	21.720
	RCV	Validation	90	0.246	28.620	21.685
	Bootstrap	Validation	90	0.150	30.107	22.302
III	LOOCV	Training	370			
		Validation	92	0.153	13.887	10.699
	CV	Validation	92	0.231	13.181	10.543
	RCV	Validation	92	0.238	13.330	10.600
	Bootstrap	Validation	92	0.192	14.175	10.986

Where: LOOCV: Leave-One-Out Cross-Validation; CV: Cross-Validation; RCV: Repeated Cross-Validation; *n*: sample size; R<sup>2</sup>: Coefficient of Determination; RMSE: Root Mean Square Error; MAE: Mean Absolute Error.

### 3.4. Current and Future Prediction of Carbon Density of Aboveground Live Biomass

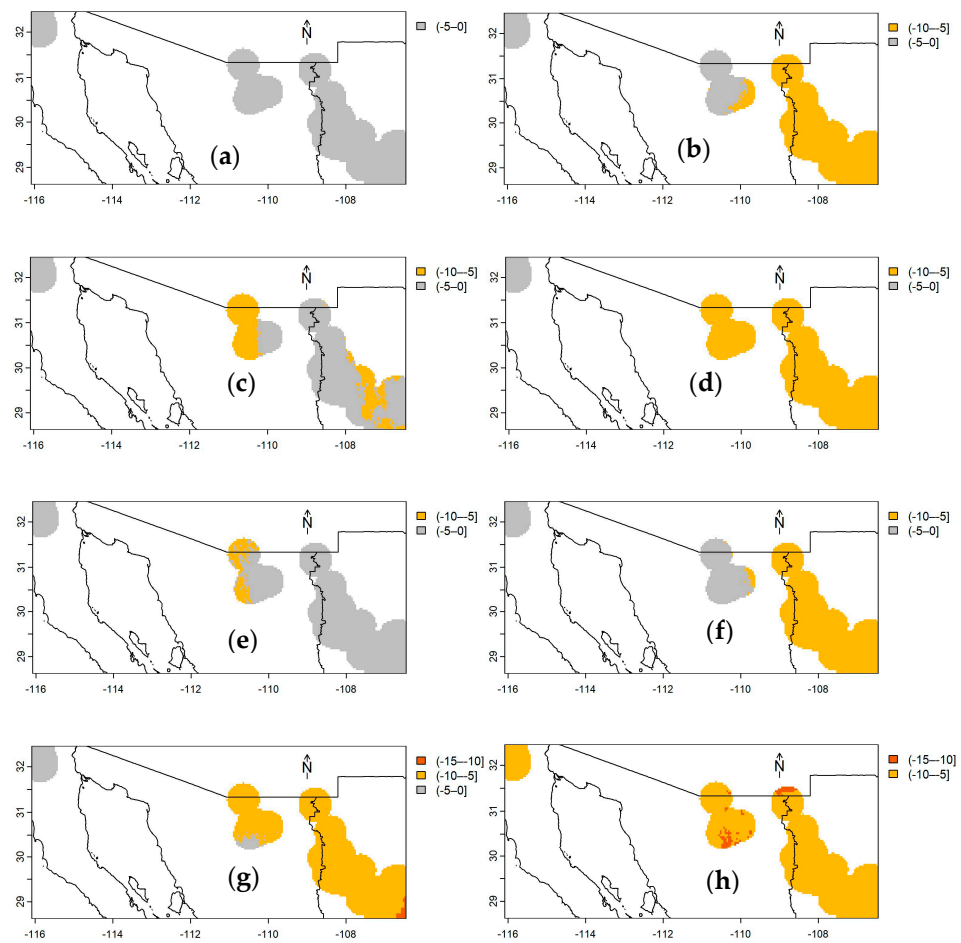
Using the bioclimatic models generated here, at the INFyS sites, predictions range from 7.48 to 34.79 Mg C ha<sup>-1</sup>, from 16.68 to 71.29 Mg C ha<sup>-1</sup>, and from 10.98 to 41.91 Mg C ha<sup>-1</sup> for strata I, II, and III, respectively (Figure 3a–c). The highest cdAGB is observed/predicted in stratum II (Figure 3b) in the central region of the country. The highest differences between the observed cdAGB and estimated cdAGB are −19 and +30, −52 and +124, −29 and +56 Mg C ha<sup>-1</sup>, respectively, for strata I, II, and III.



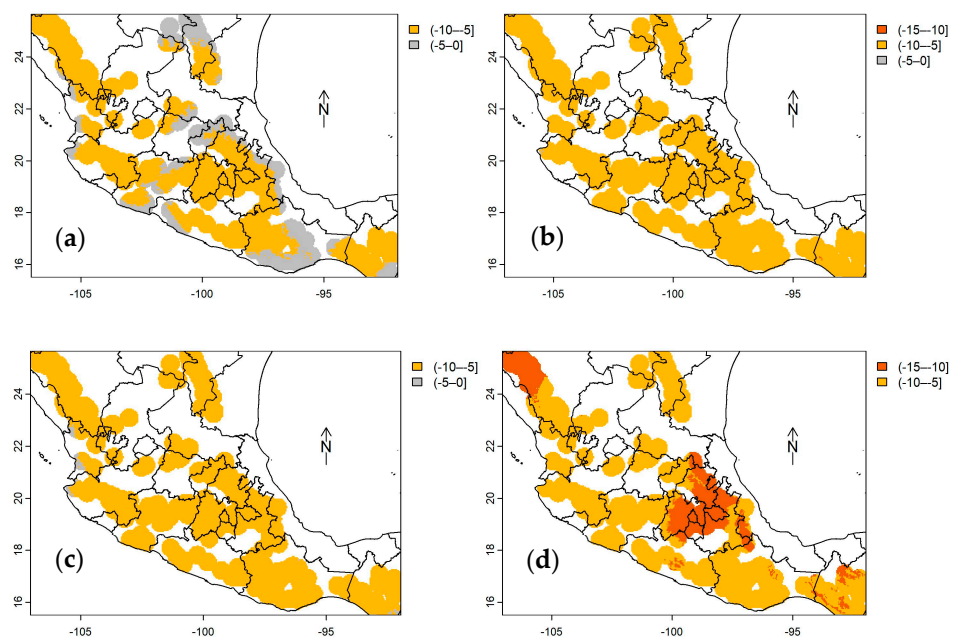
**Figure 3.** Prediction of current carbon density of aboveground live biomass in Mexican conifer forests through bioclimatic models: stratum I (a), stratum II (b), and stratum III (c). Circle size and color gradient indicate values of carbon density of aboveground live biomass ( $\text{Mg C ha}^{-1}$ ).

According to future predictions of  $\text{cdAGB}$  up to 2050 and 2070 (Figures 4–6) using the bioclimatic model for each stratum (Equations (1)–(3)), under any climate scenario (RCP), only reductions in  $\text{cdAGB}$  are expected. Forests in stratum II (Figure 5a–h, situated in the central and southern regions of the country) would be the most affected, with decreases ranging from  $-5$  to  $-10 \text{ Mg ha}^{-1}$ , potentially up to  $-20 \text{ Mg C ha}^{-1}$  by 2070, whereas those in stratum III (Figure 5a–h, SMO) would experience lesser impacts ranging from 0 to  $-5 \text{ Mg C ha}^{-1}$  (Table 4). The most significant losses of  $\text{cdAGB}$  are expected under RCP 8.5 and are anticipated to be greater by 2070.

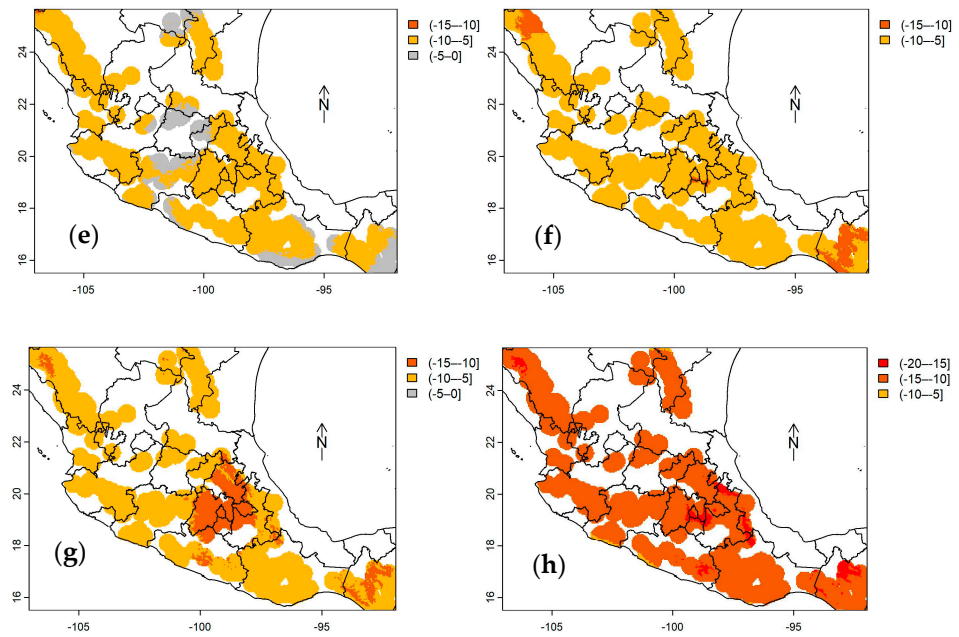




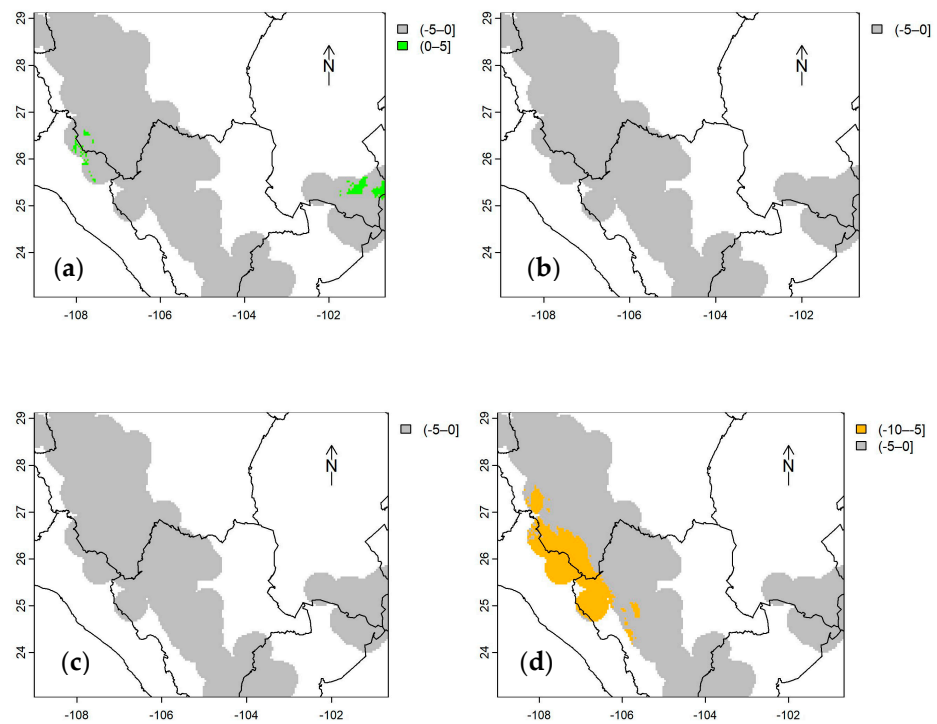
**Figure 4.** Changes in carbon density of aboveground live biomass in Mexican conifer forests under the RCP 2.6 to 8.5 scenarios (a–d) for the years 2050 and 2070 (e–h) in stratum I. Colored areas represent 40 km radius buffers around INFyS site; uncolored areas correspond to other vegetation types different from conifer forests.



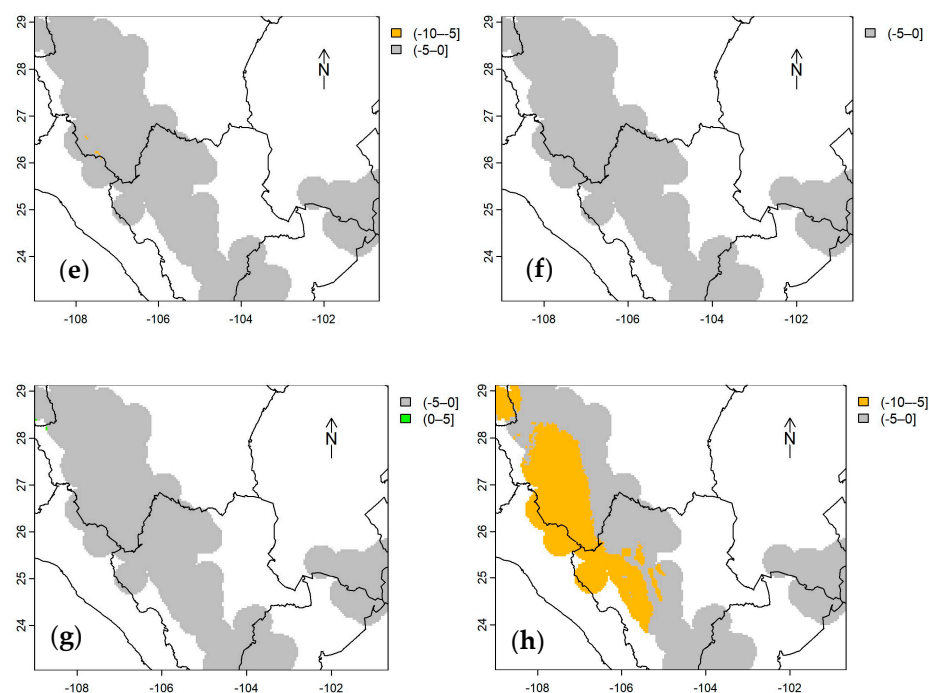
**Figure 5.** Cont.



**Figure 5.** Changes in carbon density of aboveground live biomass in Mexican conifer forests under the RCP 2.6 to 8.5 scenarios (a–d), for the years 2050 and 2070 (e–h) in stratum II. Colored areas represent 40 km radius buffers around each INFyS site; uncolored areas correspond to other vegetation types different from conifer forests.



**Figure 6.** Cont.



**Figure 6.** Changes in the carbon density of aboveground live biomass in Mexican conifer forests under the RCP 2.6 to 8.5 scenarios (a–d) for the years 2050 and 2070 (e–h) in stratum III. Colored areas represent 40 km radius buffers around each INFyS site; uncolored areas correspond to other vegetation types different from conifer forests.

**Table 4.** Number of pixels contained within the 40 km radius buffer around each sampling site of INFyS to differentiate changes in carbon density of aboveground live biomass in the conifer forests of Mexico under future climatic scenarios. Each pixel represents  $0.98 \times 0.98$  km on each side.

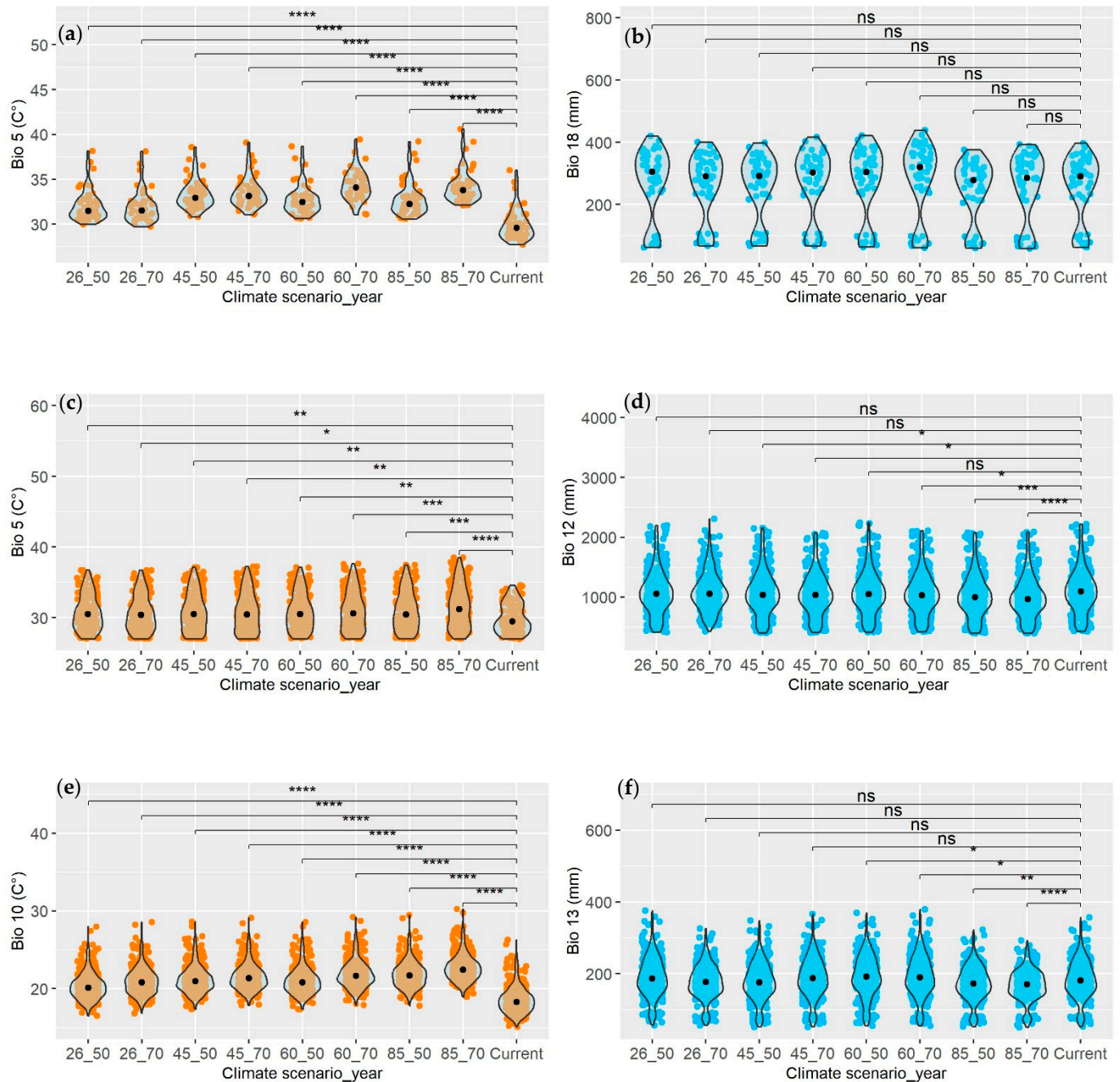
Stratum	Changes in $cd_{AGB}$	RCP 26		RCP 45		RCP 60		RCP 85	
		2050	2070	2050	2070	2050	2070	2050	2070
I	(−20–−15   <span style="color:red">■</span> )	0	0	0	0	0	0	0	0
	(−15–−10   <span style="color:red">■</span> )	0	0	0	0	0	35	0	107
	(−10–−5   <span style="color:orange">■</span> )	0	240	2361	2280	906	2885	3011	3180
	(−5–0   <span style="color:grey">■</span> )	3287	3047	926	1007	2381	367	276	0
	(0–5   <span style="color:green">■</span> )	0	0	0	0	0	0	0	0
II	(−20–−15   <span style="color:red">■</span> )	0	0	0	0	0	0	0	1148
	(−15–−10   <span style="color:red">■</span> )	0	30	6	1526	0	3928	4796	22,466
	(−10–−5   <span style="color:orange">■</span> )	17,750	19,473	23,821	22,317	23,571	19,912	19,047	229
	(−5–0   <span style="color:grey">■</span> )	6093	4340	16	0	272	3	0	0
	(0–5   <span style="color:green">■</span> )	0	0	0	0	0	0	0	0
III	(−20–−15   <span style="color:red">■</span> )	0	0	0	0	0	0	0	0
	(−15–−10   <span style="color:red">■</span> )	0	0	0	0	0	0	0	0
	(−10–−5   <span style="color:orange">■</span> )	0	6	0	0	0	0	1290	3281
	(−5–0   <span style="color:grey">■</span> )	9680	9819	9825	9825	9825	9822	8535	6544
	(0–5   <span style="color:green">■</span> )	145	0	0	0	0	3	0	0

Observed carbon density of aboveground live biomass ( $Mg\ C\ ha^{-1}$ ); RCP = Representative Concentration Pathway. The color of the box in column two corresponds to the color of the pixel in Figures 3–5.

### 3.5. Evaluation of Climate Projections on Variables Predicting $cd_{AGB}$

The Wilcoxon test provided sufficient evidence ( $p < 0.0001$ ) to reject the null hypothesis ( $H_0$ ) of equal medians between the current Bio and the same Bio under a future climate scenario. In all cases, the median of the estimated temperature Bios for 2050 and 2070, projected by three General Circulation Models (GCMs), in any climate scenario (RCP; left, Figure 7), will be higher than the current median (Table 2). Generally, the temperature

is expected to increase by 2.66 °C (2050) and 3.36 °C (2070) compared to the present (Figure 7a,c,e). The coniferous areas in stratum II are predicted to be vulnerable due to a likely increase of +2.7 °C by 2050, whereas the less vulnerable areas will be in stratum III (+2.5 °C).



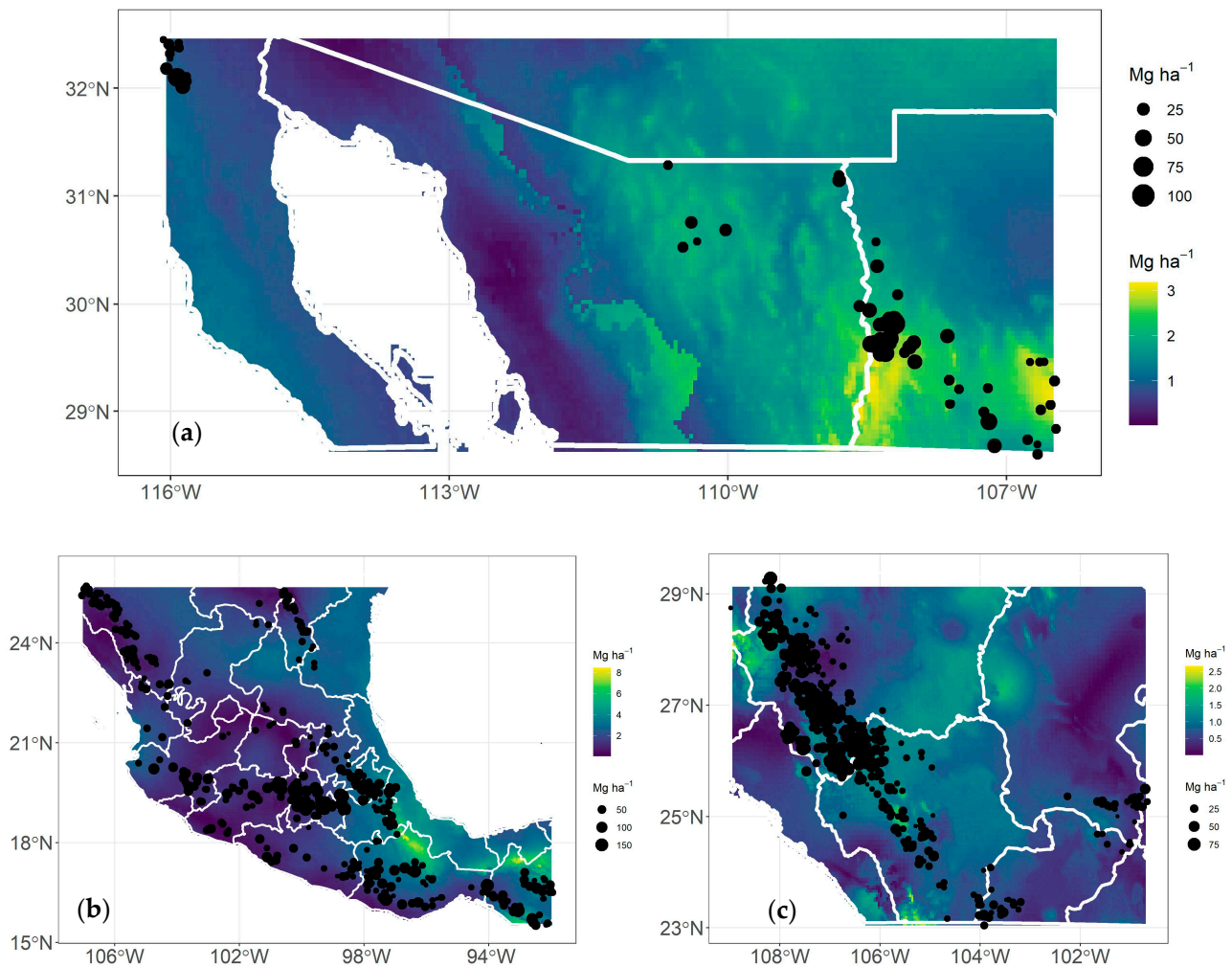
**Figure 7.** Wilcoxon test for comparing medians of the current variable with each climate scenario, in strata I (a,b), II (c,d), and III (e,f). Bio 05: Max Temperature of Warmest Month (°C); Bio 10: Mean Temperature of Warmest Quarter (°C); Bio 12: Annual Precipitation (mm); Bio 13: Precipitation of Wettest Month (mm); Bio 18: Precipitation of Warmest Quarter (mm). Significance levels: ns (Not significant), \* (Significant at 0.05%), \*\* (Significant at 1%), \*\*\* (Significant at 0.1%), \*\*\*\* (Significant at 0.01%).

Generally, the test demonstrated that in the coniferous forests of Mexico, precipitation levels in 2050 and 2070 could statistically be the same ( $p < 0.05$ ) as those currently recorded in stratum I (Figure 7b). In stratum II, precipitation is projected to decrease ( $p < 0.0001$ ) by 5.3% (2050) and 6.4% (2070) (Figure 7d), while in stratum III, it could either increase or



decrease (Figure 7f). When analyzed individually (Current vs. Bio-RCP-Year), significant differences exist only for precipitation variables (right, Figure 7) and not for temperature variables (left, Figure 7).

The uncertainty (represented by the standard error) estimated for  $_{cd}AGB$  shown here (Figure 8), for the most critical scenario (RCP 85 | 2070), indicates that the standard error ranges from 2.5 Mg C ha<sup>-1</sup> (stratum III) to 6 Mg C ha<sup>-1</sup> (stratum II), well below the RMSE (Table 3) estimated with independent data. This uncertainty is similar in less critical climatic scenarios (RCP 26 | 2050).



**Figure 8.** Estimated uncertainty (standard error) of carbon density of aboveground live biomass in Mexican conifer forests, for strata I (a), II (b), and III (c) under RCP 85 and for the year 2070.

#### 4. Discussion

The selection of  $_{cd}AGB$  predictors through automated algorithms (stepwise, machine learning, neural networks, etc.) is generally efficient. These algorithms have been tested in natural forests [44,45], tropical rainforests [46], and even in plantations [19]. Although the variables selected by these algorithms are statistically significant,  $p < 0.05$  [36], the models generated here exhibited multicollinearity effects ( $VIF > 10$ ); consequently, these models had to be evaluated to mitigate this effect and enhance the accuracy of the predictions.

Some authors [47] have used linear procedures (lm) for predicting NPP (Net Primary Production) in grasslands, with favorable results. We tested this technique; however, it was demonstrated that in this type of study, it is difficult to meet all the assumptions of a regression model ( $\varepsilon_i \sim N(0, \sigma^2)$ ), which is why the “glm” procedure was ultimately employed, as has been done in such studies [2,9]. In addition to these procedures, the



Random Forest [8,48,49] and Bayesian models [20] have also been used for predicting AGB (above-ground biomass) from temperature and precipitation variables.

#### 4.1. Predictor Variables of Aboveground Biomass

In this study, the algorithms selected both temperature variables (Bio5 and Bio10) and precipitation variables (Bio12, Bio13, and Bio18) as the best predictors of  $_{cd}AGB$ . Temperature variables were the most important in the model (contributing 8 to 10% to the pseudo  $R^2$ ) for strata I and II (Table 1, Figure 2a,b), but not for stratum III. According to some authors [21,47], on a global scale, precipitation and temperature variables are the best predictors of AGB. Specifically, annual mean temperature (Bio1) and temperature of the warmest quarter (Bio10) are climatic variables associated with biomass distribution on broad scales. Metrics demonstrate that temperatures appear to be more important than precipitation variables [28].

It has been demonstrated that the bioclimatic variables of temperature (Bio1 and Bio5) and precipitation (Bio12) are associated with the accumulation of AGB in forests [20], boreal ecosystems [19], temperate seasonal ecosystems [18], tropical rainforests [50], and tropical seasonal ecosystems [4,5]. As can be observed, Bio5 and Bio12 (Appendix A) are good predictors of AGB across different types of ecosystems. For instance, a study conducted in the SMO (stratum II of this same study) indicates that average temperature (Bio1) is the most important predictor for AGB in temperate forests [25].

In Australian forests, encompassing 15 types of forests predominantly dominated by eucalypts [8], it has been demonstrated that climatic variables are better predictors of AGB than soil variables, with Bio 9 (Mean Temperature of Driest Quarter) being the most important variable. Regardless of the metrics, as in our study, temperature variables appear to be the most important for predicting AGB (Table 1).

However, the relationship between bioclimatic variables and AGB is entirely dependent on the type of ecosystem, the species, and the region of the world. For this reason, other authors emphasize that the mean annual precipitation (MAP) has a relatively greater importance (0.19%) than the mean annual temperature (MAT) (0.05%) for predicting AGB in *Larix* plantations in northern and northeastern China. Furthermore, its importance is also dependent on the model structure [19].

Continuing with the previous narrative, the relationship between precipitation and AGB can be complex, as different responses may be observed depending on the type of forest and climatic conditions. This variable significantly influences the accumulation of different components of AGB (branches, stems, roots, and needles) in conifer plantations. Therefore, it is essential to consider it in predictive models and the evaluation of the climate-forest relationship [12]. However, climatic variables such as temperature and precipitation together can improve AGB estimates [21]. In tropical forests [51], 13 predictor variables of AGB were used, including geographical, topographical, hydrological, soil, and even species-related variables (e.g., coverage). They found that the relative influence of MAP on AGB is 37.6%, making it the most important, while MAT has a relative influence of less than 1%.

#### 4.2. Correlation Between Bioclimatic Variables and Carbon Density

The correlation of  $_{cd}AGB$  with temperature variables (Bio 5 and Bio 10) in temperate forests of Mexico is negative but positive with precipitation variables (Table 1). Similar findings were reported by [23], who observed a negative correlation ( $-0.46 > r < -0.63$ ;  $-0.43 > r < -0.60$ ) between the stem biomass of *Larix gmelinii* and *Betula platyphylla* with MAT. Likewise, other studies have demonstrated that MAT is negatively correlated with AGB, either at the species level [12] or at the stand level [36].

Similar to this study, in temperate and dry forests, a positive correlation between  $_{cd}AGB$  and MAP has been observed [27]. This same relationship is found in other studies; for instance, [23] discovered that MAP positively correlates with the stem biomass of *Larix gmelinii* ( $0.84 > r < 0.92$ ) and *Betula platyphylla* ( $0.76 > r < 0.88$ ). Additionally, [12] observed

that MAP positively and significantly ( $p < 0.05$ ) correlates with the AGB of *Pinus koraiensis* Siebold & Zucc., *Larix olgensis* A. Henry, and *Pinus sylvestris* var. *mongolica* Litv.

Furthermore, the study conducted by [28] reveals that, on a global scale (>6200 forests and 61 countries), MAT is positively correlated with foliage biomass, although the geographical patterns of correlation are inconsistent. The authors of [14] found that while temperature correlates positively in boreal forests, the opposite occurs in tropical forests. Studies conducted by [4] in boreal forests demonstrate that MAT can explain ( $R^2$ ) between 26% and 45% of carbon density and is positively correlated; whereas MAP can explain between 28% and 67% of carbon density (both aboveground and belowground); however, the correlation between these two variables is positive when precipitation is between 0 and 1000 mm and negative when it exceeds 1000 mm.

In contrast to this study, in boreal and temperate forests, a positive relationship has been found between  $_{cd}AGB$  and MAT [18], but a negative one in humid regions [27].

#### 4.3. Predictive Capacity of Bioclimatic Models

Model validation is crucial for assessing the predictive capacity of a model based on new data. In reality, within this context (AGB–climatic predictor relationship), few studies undertake this process [19,48,52,53]. As is known, when generating a model using the “glm” procedure, statistics such as  $R^2$ , RMSE, and MAE, are not computed. Upon validating our models, we were able to calculate these metrics and evaluate the predictive capacity of each model. We observed that bioclimatic variables can explain up to 22% of  $_{cd}AGB$  in these types of forests (Table 3), a reasonably significant value at the eco-region level [4], but not at the species level [12,23], where variables can explain up to 84% of AGB at this scale.

In general, the “cross-validation” technique has been the most commonly used to validate models for estimating AGB [19,36,53,54]; in this study, we used it along with three other techniques (Table 3). It is noteworthy that when dealing with climatic predictors, these can explain around 20% (Table 3), whereas predicting AGB from predictors derived from vegetation indices, e.g., normalized difference vegetation index (NDVI), spectral information [53], or satellite optical images and unmanned aerial vehicles [54], can explain ( $R^2$ ) up to 80% of AGB. The inclusion of different predictor variables such as MAP, MAT, clay content, pH, dryness index, and stand age can explain up to 44.4% of  $_{cd}AGB$  in temperate forests [4].

However, exclusive stand predictors (diameter at breast height, age, and stand density) can explain up to 98% of the AGB variance [19]. The RMSE metric is entirely dependent on the units and scale of the dependent variables, which is why such distant differences are observed across studies.

#### 4.4. Current and Future Projection of $_{cd}AGB$

Under any climate scenario (RCP—year), our models predict losses in  $_{cd}AGB$  ranging from 5 Mg C ha<sup>-1</sup> (2050) to 20 Mg C ha<sup>-1</sup> by 2070 (Figures 4–6) in Mexico’s coniferous forests. Globally, positive changes in Total Carbon Density (TCD) are projected for temperate forests, averaging 2.23 Mg C ha<sup>-1</sup> (RCP 26, 45, and 85; 2050) and 1.99 Mg C ha<sup>-1</sup> by 2070. Specifically for Mexico, these authors [4] predict changes of  $\pm 20$  Mg C ha<sup>-1</sup>. It is important to note that, for the country, only two plots were considered in [4], whereas our study was conducted at a finer scale, generating models from  $n = 48$  to  $n = 370$  (Table 2).

A study conducted by [55] under various simulation scenarios, altering temperature and precipitation, in Yunnan Province, China, suggests that the combined effects of these variables are more complex than anticipated. These effects can result in both gains and losses (as observed in this study) in carbon sequestration across different forest types, attributed to decreased precipitation and increased temperature. Our study shows a decrease in  $_{cd}AGB$ , primarily due to a temperature increase of 1 to 3 °C and a precipitation decrease of approximately 10%. Nearly three decades ago [56], the vulnerability of Mexico’s forests to climate change was assessed, revealing that under these conditions (+2 °C and

–10% precipitation), the area of humid and dry temperate forests would significantly decrease (to less than half of their current size).

In a study conducted in the Brazilian Atlantic Forest (AF) [57], it was found that in 34.7% of the existing forest fragments, AGB could increase, while in 2.6%, it could decrease by the year 2100. Models predict an 8.5% increase in total carbon stock; additionally, 76.9% of AF would be suitable for a potential increase in AGB by 2100 under RCP 4.5, solely due to climate change. This contrasts with findings here, possibly due to differences in forest types and geographical location, but is similar to what was found by [36] in subtropical evergreen forests in China, showing a decrease in AGB by 2050–2070, varying according to different climate scenarios (RCP 2.6 > RCP 4.5 > RCP 6.0 > RCP 8.5).

## 5. Conclusions

The relationships between  $c_d$ AGB and climate are more complex than they may initially appear. Bioclimatic variables, especially those related to temperature, have proven to be significant predictors of  $c_d$ AGB in the developed models and can explain up to 19% of  $c_d$ AGB. Bio 5 (Max Temperature of Warmest Month) emerged as the most robust predictor. Predictions using bioclimatic models suggest that all strata of the country's coniferous forests, under any climate scenario (RCP—Year), will experience declines in  $c_d$ AGB (in the absence of anthropogenic activities) by 2050 and 2070, particularly under the RCP 8.5 scenario. It is expected that forests in stratum II will be the most affected, with significant reductions that could reach up to  $-20 \text{ Mg C ha}^{-1}$  by the year 2070. The temperature projected by the GCMs for 2050 and 2070 will be significantly higher than current levels, with increases of up to  $3.55 \text{ }^\circ\text{C}$  in stratum I by 2070. Precipitation could remain unchanged in stratum I, decrease ( $-10\%$ ) in stratum II, and vary ( $\pm 10\%$ ) in stratum III. These future climate projections are expected to lead to a redistribution of  $c_d$ AGB in Mexican forests. The conclusions suggest an urgent need for adaptation and mitigation strategies to conserve biodiversity and ecosystem services provided by conifer forests in Mexico. Forest management should consider not only biodiversity conservation but also the carbon storage capacity of these ecosystems.

**Author Contributions:** Conceptualization, J.M.-G. and C.S.-G.; methodology, J.M.-G. and J.Á.V.-Q.; software, C.S.-G.; validation, E.H.C.-O., C.F.-L. and F.A.; formal analysis, J.M.-G.; investigation, F.P.-P. and E.E.V.-G.; resources, A.Z.-G. and L.S.-D.; data curation, C.S.-G., M.G.-G. and F.A.; writing—original draft preparation, C.S.-G.; writing—review and editing, E.H.C.-O., A.Z.-G. and E.E.V.-G.; visualization, L.S.-D. and M.G.-G.; supervision, J.M.-G.; project administration, J.M.-G. All authors have read and agreed to the published version of the manuscript.

**Funding:** This research was funded by AUTONOMOUS AGRARIAN UNIVERSITY ANTONIO NARRO, grant number 38111425103001-2185.

**Data Availability Statement:** Data are contained within the article.

**Acknowledgments:** The authors are grateful to the AUTONOMOUS AGRARIAN UNIVERSITY ANTONIO NARRO, for funding all stages of this study through Project No 38111425103001-2185.

**Conflicts of Interest:** The authors declare no conflicts of interest. The funders had no role in the design of the study; in the collection, analyses, or interpretation of data; in the writing of the manuscript; or in the decision to publish the results.

### Appendix A. Comprehensive Dataset of Physical and Biological Biomass and Carbon Content Parameters in Mexico's National Forest Inventory

#	Name	Short Name	Unit
1	Identification (Cluster no.) *	ID	
2	Type* (Conifers forests) *	Type	
3	Tenure	Tenure	
4	Slope	Slope	deg
5	DEPTH, soil	Depth soil	m
6	Structural richness	Structural rich	
7	Tree richness	Tree rich	
8	Number of stumps	Stumps	#
9	Biomass, aboveground	Biom abovegr	t/ha
10	Biomass, belowground	Biom belowgr	t/ha
11	Biomass, total	Biom total	t/ha
12	Carbon, aboveground *	C abovegr	t/ha
13	Carbon, belowground	C belowgr	t/ha
14	Soil carbon stock	C stock	t/ha
15	Fires index	Fires	
16	Pests index	Pests	
17	Temperature, air, annual mean	MAAT	°C
18	Precipitation, annual mean	MAP	mm
19	Longitude *	Longitude	
20	Latitude *	Latitude	
21	Trees, diameter at breast height	DBH	cm
22	Height	Height	m

\* Selected parameters for data analysis in the present study.

### Appendix B. Bioclimatic Variables

Variable	Description	Units	Scale
Bio 1	Annual Mean Temperature	°C	Annual
Bio 2	Mean Diurnal Range (max temp–min temp)	°C	Monthly
Bio 3	Isothermality (Bio02/Bio07) ( $\times 100$ )	%	Annual
Bio 4	Temperature Seasonality (standard deviation $\times 100$ )	%	Annual
Bio 05	Max Temperature of Warmest Month	°C	Monthly
Bio 06	Min Temperature of Coldest Month	°C	Monthly
Bio 07	Temperature Annual Range (Bio5–Bio6)	°C	Annual
Bio 08	Mean Temperature of Wettest Quarter	°C	Quarterly
Bio 09	Mean Temperature of Driest Quarter	°C	Quarterly
Bio 10	Mean Temperature of Warmest Quarter	°C	Quarterly
Bio 11	Mean Temperature of Coldest Quarter	°C	Quarterly
Bio 12	Annual Precipitation	mm	Annual
Bio 13	Precipitation of Wettest Month	mm	Monthly
Bio 14	Precipitation of Driest Month	mm	Monthly
Bio 15	Precipitation Seasonality (Coefficient of variation)	%	Quarterly
Bio 16	Precipitation of Wettest Quarter	mm	Quarterly
Bio 17	Precipitation of Driest Quarter	mm	Quarterly
Bio 18	Precipitation of Warmest Quarter	mm	Quarterly
Bio 19	Precipitation of Coldest Quarter	mm	Quarterly

### References

1. FAO. *El Estado de Los Bosques Del Mundo 2022*; FAO: Rome, Italy, 2022.
2. Arasa-Gisbert, R.; Vayreda, J.; Román-Cuesta, R.M.; Villela, S.A.; Mayorga, R.; Retana, J. Forest Diversity Plays a Key Role in Determining the Stand Carbon Stocks of Mexican Forests. *For. Ecol. Manag.* **2018**, *415–416*, 160–171. [[CrossRef](#)]
3. Rodríguez-Veiga, P.; Saatchi, S.; Tansey, K.; Balzter, H. Magnitude, Spatial Distribution and Uncertainty of Forest Biomass Stocks in Mexico. *Remote Sens. Environ.* **2016**, *183*, 265–281. [[CrossRef](#)]

4. Guo, Y.; Peng, C.; Trancoso, R.; Zhu, Q.; Zhou, X. Stand Carbon Density Drivers and Changes under Future Climate Scenarios across Global Forests. *For. Ecol. Manag.* **2019**, *449*, 117463. [[CrossRef](#)]
5. Ma, Y.; Eziz, A.; Halik, Ü.; Abliz, A.; Kurban, A. Precipitation and Temperature Influence the Relationship between Stand Structural Characteristics and Aboveground Biomass of Forests—A Meta-Analysis. *Forests* **2023**, *14*, 896. [[CrossRef](#)]
6. IPCC. *Climate Change 2021—The Physical Science Basis*; Cambridge University Press: Cambridge, UK, 2021; pp. 3–32.
7. Climate Risk Profile: Mexico (2023): The World Bank Group. Washington, DC, USA. 41 p. Available online: [https://climateknowledgeportal.worldbank.org/sites/default/files/country-profiles/15634-WB\\_Mexico%20Country%20Profile-WEB%20\(2\).pdf](https://climateknowledgeportal.worldbank.org/sites/default/files/country-profiles/15634-WB_Mexico%20Country%20Profile-WEB%20(2).pdf) (accessed on 22 June 2024).
8. Bennett, A.C.; Penman, T.D.; Arndt, S.K.; Roxburgh, S.H.; Bennett, L.T. Climate More Important than Soils for Predicting Forest Biomass at the Continental Scale. *Ecography* **2020**, *43*, 1692–1705. [[CrossRef](#)]
9. Cysneiros, V.C.; Coelho de Souza, F.; Gaudi, T.D.; Pelissari, A.L.; Orso, G.A.; Machado, S.d.A.; de Carvalho, D.C.; Silveira-Filho, T.B. Integrating Climate, Soil and Stand Structure into Allometric Models: An Approach of Site-Effects on Tree Allometry in Atlantic Forest. *Ecol. Indic.* **2021**, *127*, 107794. [[CrossRef](#)]
10. Gao, J.; Zhao, P.; Shen, W.; Rao, X.; Hu, Y. Physiological Homeostasis and Morphological Plasticity of Two Tree Species Subjected to Precipitation Seasonal Distribution Changes. *Perspect. Plant Ecol. Evol. Syst.* **2017**, *25*, 1–19. [[CrossRef](#)]
11. Yuan, J.; Yan, Q.; Wang, J.; Xie, J.; Li, R. Different Responses of Growth and Physiology to Warming and Reduced Precipitation of Two Co-Existing Seedlings in a Temperate Secondary Forest. *Front. Plant Sci.* **2022**, *13*, 946141. [[CrossRef](#)]
12. Xin, S.; Wang, J.; Mahardika, S.B.; Jiang, L. Sensitivity of Stand-Level Biomass to Climate for Three Conifer Plantations in Northeast China. *Forests* **2022**, *13*, 2022. [[CrossRef](#)]
13. Eamus, D. How Does Ecosystem Water Balance Affect Net Primary Productivity of Woody Ecosystems? *Funct. Plant Biol.* **2003**, *30*, 187–205. [[CrossRef](#)]
14. Liu, Y.; Yu, G.; Wang, Q.; Zhang, Y. How Temperature, Precipitation and Stand Age Control the Biomass Carbon Density of Global Mature Forests. *Glob. Ecol. Biogeogr.* **2014**, *23*, 323–333. [[CrossRef](#)]
15. Han, S.H.; Kim, D.H.; Kim, G.N.; Lee, J.C.; Yun, C.W. Changes on Initial Growth and Physiological Characteristics of Larix Kaempferi and Betula Costata Seedlings under Elevated Temperature. *Korean J. Agric. For. Meteorol.* **2012**, *14*, 63–70. [[CrossRef](#)]
16. Devi, V.; Kaur, A.; Sethi, M.; Avinash, G. Perspective Chapter: Effect of Low-Temperature Stress on Plant Performance and Adaptation to Temperature Change. In *Plant Abiotic Stress Responses and Tolerance Mechanisms*; IntechOpen: London, UK, 2023.
17. Pan, Y.; Birdsey, R.A.; Phillips, O.L.; Jackson, R.B. The Structure, Distribution, and Biomass of the World’s Forests. *Annu. Rev. Ecol. Evol. Syst.* **2013**, *44*, 593–622. [[CrossRef](#)]
18. Keith, H.; Mackey, B.G.; Lindenmayer, D.B. Re-Evaluation of Forest Biomass Carbon Stocks and Lessons from the World’s Most Carbon-Dense Forests. *Proc. Natl. Acad. Sci. USA* **2009**, *106*, 11635–11640. [[CrossRef](#)] [[PubMed](#)]
19. He, X.; Lei, X.; Zeng, W.; Feng, L.; Zhou, C.; Wu, B. Quantifying the Effects of Stand and Climate Variables on Biomass of Larch Plantations Using Random Forests and National Forest Inventory Data in North and Northeast China. *Sustainability* **2022**, *14*, 5580. [[CrossRef](#)]
20. Chen, X.; Luo, M.; Larjavaara, M. Effects of Climate and Plant Functional Types on Forest Above-Ground Biomass Accumulation. *Carbon Balance Manag.* **2023**, *18*, 5. [[CrossRef](#)]
21. Dai, L.; Ke, X.; Guo, X.; Du, Y.; Zhang, F.; Li, Y.; Li, Q.; Lin, L.; Peng, C.; Shu, K.; et al. Responses of Biomass Allocation across Two Vegetation Types to Climate Fluctuations in the Northern Qinghai–Tibet Plateau. *Ecol. Evol.* **2019**, *9*, 6105–6115. [[CrossRef](#)] [[PubMed](#)]
22. Girón-Gutiérrez, D.; Méndez-González, J.; Osorno-Sánchez, T.G.; Cerano-Paredes, J.; Soto-Correa, J.C.; Cambrón-Sandoval, V.H. Climate as a Driver of Aboveground Biomass Density Variation: A Study of Ten Pine Species in Mexico. *Forests* **2024**, *15*, 1160. [[CrossRef](#)]
23. Khan, D.; Muneer, M.A.; Nisa, Z.U.; Shah, S.; Amir, M.; Saeed, S.; Uddin, S.; Munir, M.Z.; Lushuang, G.; Huang, H. Effect of Climatic Factors on Stem Biomass and Carbon Stock of Larix Gmelinii and Betula Platyphylla in Daxing’anling Mountain of Inner Mongolia, China. *Adv. Meteorol.* **2019**, 1–10. [[CrossRef](#)]
24. David, H.C.; de Araújo, E.J.G.; Morais, V.A.; Scolforo, J.R.S.; Marques, J.M.; Péllico Netto, S.; MacFarlane, D.W. Carbon Stock Classification for Tropical Forests in Brazil: Understanding the Effect of Stand and Climate Variables. *For. Ecol. Manag.* **2017**, *404*, 241–250. [[CrossRef](#)]
25. López-Serrano, P.M.; Domínguez, J.L.C.; Corral-Rivas, J.J.; Jiménez, E.; López-Sánchez, C.A.; Vega-Nieva, D.J. Modeling of Aboveground Biomass with Landsat 8 Oli and Machine Learning in Temperate Forests. *Forests* **2020**, *11*, 11. [[CrossRef](#)]
26. Rezashobairi, S.; Lin, H.; Usoltsev, V.; Osmirko, A.; Tsepordey, I.; Ye, Z.; Anees, S. A Comparative Pattern for Populus Spp. and Betula Spp. Stand Biomass in Eurasian Climate Gradients. *Croat. J. For. Eng.* **2022**, *43*, 457–467. [[CrossRef](#)]
27. Stegen, J.C.; Swenson, N.G.; Enquist, B.J.; White, E.P.; Phillips, O.L.; Jørgensen, P.M.; Weiser, M.D.; Monteagudo Mendoza, A.; Núñez Vargas, P. Variation in Above-Ground Forest Biomass across Broad Climatic Gradients. *Glob. Ecol. Biogeogr.* **2011**, *20*, 744–754. [[CrossRef](#)]
28. Reich, P.B.; Luo, Y.; Bradford, J.B.; Poorter, H.; Perry, C.H.; Oleksyn, J. Temperature Drives Global Patterns in Forest Biomass Distribution in Leaves, Stems, and Roots. *Proc. Natl. Acad. Sci. USA* **2014**, *111*, 13721–13726. [[CrossRef](#)]
29. Ellis, C.J. Climate Change, Bioclimatic Models and the Risk to Lichen Diversity. *Diversity* **2019**, *11*, 54. [[CrossRef](#)]



30. Gernandt, D.S.; Pérez-De La Rosa, J.A. Biodiversity of Pinophyta (Conifers) in Mexico. *Rev. Mex. Biodivers.* **2014**, *85*, 215–223. [[CrossRef](#)]
31. Rzedowski, J.; Huerta, L. *Vegetación de México*; Editorial Limusa: Ciudad de México, Mexico, 2006.
32. Granados-Sánchez, D.; López-Ríos, G.F.; Hernández-García, M.A. Ecología Y Silvicultura Bosques Templados. *Rev. Chapingo Ser. Cienc. For. Y Ambiente* **2007**, *13*, 67–80.
33. Challenger, A. *Utilización y Conservación de Los Ecosistemas Terrestres de México*; Instituto de Biología: Distrito Federal, Mexico, 1998; 847p, ISBN 970-9000-02-0. Available online: <https://biblioteca.ecosur.mx/cgi-bin/koha/opac-detail.pl?biblionumber=23389> (accessed on 12 August 2024).
34. Grupo Intergubernamental de Expertos sobre el Cambio Climático (IPCC). Orientación Sobre las Buenas Prácticas para uso de la Tierra, Cambio de uso de la Tierra y Silvicultura. Available online: [https://www.ipcc-nggip.iges.or.jp/public/gpglulucf/gpglulucf\\_languages.html](https://www.ipcc-nggip.iges.or.jp/public/gpglulucf/gpglulucf_languages.html) (accessed on 12 August 2024).
35. Fick, S.E.; Hijmans, R.J. WorldClim 2: New 1-km Spatial Resolution Climate Surfaces for Global Land Areas. *Int. J. Climatol.* **2017**, *37*, 4302–4315. [[CrossRef](#)]
36. Li, Y.; Li, M.; Wang, Y. Forest Aboveground Biomass Estimation and Response to Climate Change Based on Remote Sensing Data. *Sustainability* **2022**, *14*, 14222. [[CrossRef](#)]
37. Hijmans, R.J. raster: Geographic Data Analysis and Modeling. R package version 3.6-26. 2023. Available online: <https://CRAN.R-project.org/package=raster> (accessed on 6 October 2024).
38. Lê, S.; Josse, J.; Rennes, A.; Husson, F. FactoMineR: An R Package for Multivariate Analysis. *J. Stat. Softw.* **2008**, *25*, 1–18. [[CrossRef](#)]
39. Corcoran, D.C. GeoStratR: Simple Spatial Stratification of Rasters. 2024. Available online: <https://sustainscapes.github.io/GeoStratR/> (accessed on 12 August 2024).
40. Kuhn, M. Building predictive models in R using the caret package. *J. Stat. Softw.* **2008**, *28*, 1–26. [[CrossRef](#)]
41. Grömping, U. Relative Importance for Linear Regression in R: The Package Relaimpo. *J. Stat. Softw.* **2006**, *17*, 1–27. [[CrossRef](#)]
42. IPCC. *Climate Change 2013: The Physical Science Basis. Contribution of Working Group I to the Fifth Assessment Report of the Intergovernmental Panel on Climate Change*; Stocker, T.F., Qin, D., Plattner, G.-K., Tignor, M., Allen, S.K., Boschung, J., Nauels, A., Xia, Y., Bex, V., Midgley, P.M., Eds.; Cambridge University Press: Cambridge, UK, 2013; p. 1535.
43. R Core Team. *R: A Language and Environment for Statistical Computing*; R Foundation for Statistical Computing: Vienna, Austria, 2024.
44. Luo, M.; Wang, Y.; Xie, Y.; Zhou, L.; Qiao, J.; Qiu, S.; Sun, Y. Combination of Feature Selection and Catboost for Prediction: The First Application to the Estimation of Aboveground Biomass. *Forests* **2021**, *12*, 216. [[CrossRef](#)]
45. Bjork, S.; Anfinsen, S.N.; Naesset, E.; Gobakken, T.; Zahabu, E. On the Potential of Sequential and Nonsequential Regression Models for Sentinel-1-Based Biomass Prediction in Tanzanian Miombo Forests. *IEEE J. Sel. Top. Appl. Earth Obs. Remote Sens.* **2022**, *15*, 4612–4639. [[CrossRef](#)]
46. Ortiz-Reyes, A.D.; Valdez-Lazalde, J.R.; Ángeles-Pérez, G.; de los Santos-Posadas, H.M.; Schneider, L.; Aguirre-Salado, C.A.; Peduzzi, A. Synergy of Landsat, Climate and LiDAR Data for Aboveground Biomass Mapping in Medium-Stature Tropical Forests of the Yucatan Peninsula, Mexico. *Rev. Chapingo Ser. Cienc. For. Ambiente* **2021**, *27*, 383–400. [[CrossRef](#)]
47. Zhang, H.; Feng, Z.; Shen, C.; Li, Y.; Feng, Z.; Zeng, W.; Huang, G. Relationship between the Geographical Environment and the Forest Carbon Sink Capacity in China Based on an Individual-Tree Growth-Rate Model. *Ecol. Indic.* **2022**, *138*, 108814. [[CrossRef](#)]
48. Cartus, O.; Kellndorfer, J.; Walker, W.; Franco, C.; Bishop, J.; Santos, L.; Fuentes, J.M.M. A National, Detailed Map of Forest Aboveground Carbon Stocks in Mexico. *Remote Sens.* **2014**, *6*, 5559–5588. [[CrossRef](#)]
49. Yan, M.; Xia, Y.; Yang, X.; Wu, X.; Yang, M.; Wang, C.; Hou, Y.; Wang, D. Biomass Estimation of Subtropical Arboreal Forest at Single Tree Scale Based on Feature Fusion of Airborne LiDAR Data and Aerial Images. *Sustainability* **2023**, *15*, 1676. [[CrossRef](#)]
50. Chen, L.; Ren, C.; Zhang, B.; Wang, Z.; Xi, Y. Estimation of Forest Above-Ground Biomass by Geographically Weighted Regression and Machine Learning with Sentinel Imagery. *Forests* **2018**, *9*, 582. [[CrossRef](#)]
51. Adhikari, H.; Heiskanen, J.; Siljander, M.; Maeda, E.; Heikinheimo, V.; Pellikka, P.K.E. Determinants of Aboveground Biomass across an Afromontane Landscape Mosaic in Kenya. *Remote Sens.* **2017**, *9*, 827. [[CrossRef](#)]
52. Zhang, L.; Jiang, Y.; Zhao, S.; Dong, M.; Chen, H.Y.H.; Kang, X. Different Responses of the Radial Growth of Conifer Species to Increasing Temperature along Altitude Gradient: *Pinus Tabulaeformis* in the Helan Mountains (Northwestern China). *Pol. J. Ecol.* **2016**, *64*, 509–525. [[CrossRef](#)]
53. Opelele, O.M.; Yu, Y.; Fan, W.; Chen, C.; Kachaka, S.K. Biomass Estimation Based on Multilinear Regression and Machine Learning Algorithms in the Mayombe Tropical Forest, in the Democratic Republic of Congo. *Appl. Ecol. Environ. Res.* **2021**, *19*, 359–377. [[CrossRef](#)]
54. Wang, Z.; Yi, L.; Xu, W.; Zheng, X.; Xiong, S.; Bao, A. Integration of UAV and GF-2 Optical Data for Estimating Aboveground Biomass in Spruce Plantations in Qinghai, China. *Sustainability* **2023**, *15*, 9700. [[CrossRef](#)]
55. Zhou, R.; Zhang, Y.; Peng, M.; Jin, Y.; Song, Q. Effects of Climate Change on the Carbon Sequestration Potential of Forest Vegetation in Yunnan Province, Southwest China. *Forests* **2022**, *13*, 306. [[CrossRef](#)]

- 
56. Villers-Ruiz, L.; Trejo-Vazquez, I. Climate Research Clim Res Assessment of the Vulnerability of Forest Ecosystems to Climate Change in Mexico. *Clim. Res.* **1997**, *9*, 87–93. [[CrossRef](#)]
  57. Ferreira, I.J.M.; Campanharo, W.A.; Fonseca, M.G.; Escada, M.I.S.; Nascimento, M.T.; Villela, D.M.; Brancalion, P.; Magnago, L.F.S.; Anderson, L.O.; Nagy, L.; et al. Potential Aboveground Biomass Increase in Brazilian Atlantic Forest Fragments with Climate Change. *Glob. Chang. Biol.* **2023**, *29*, 3098–3113. [[CrossRef](#)]

**Disclaimer/Publisher’s Note:** The statements, opinions and data contained in all publications are solely those of the individual author(s) and contributor(s) and not of MDPI and/or the editor(s). MDPI and/or the editor(s) disclaim responsibility for any injury to people or property resulting from any ideas, methods, instructions or products referred to in the content.